ISBN: 978-3-95450-208-0 doi:10.18429/JACoW-IPAC2019-THPRB050

LLRF SYSTEM MODELLING AND CONTROLLER DESIGN IN UED*

Y. Q. Li, K. Fan†, Y. Song,
Huazhong University of Science and Technology, Wuhan, China

Abstract

In the Ultrafast Electron Diffraction (UED) facility for investigating material structure, voltage drifts of amplitude and phase in cavity have different effects on beam quality. So, it is critical for pump-probe experiments in the UED to keep accurate synchronization between the laser and electron. To achieve the desired 50fs resolution, the Low-Level Radio Frequency (LLRF) controller in S-band normal conducting cavity needs to satisfy the stability of ±0.01% (rms) for the amplitude and ±0.01° (rms) for the phase. Then we can study the performance of the RF control system by simulating the LLRF system. In the simulation program, feedback, feed-forward algorithms, and beam current variations can be simulated in a MATLAB/Simulink environment. This paper shows that a LLRF system controller design can meet the necessary requirements of the field regulation and implement the algorithms.

INSTRODUCTION

The Ultrafast Electron Diffraction (UED) facility being designed will provides several femtosecond electron beams for the time-resolved experiments of material structures in pump-probe configurations. The bunch is generated by impacting a commercial Ti:sapphire laser onto a photocathode in a 1.4 cell RF gun that accelerates electrons up to 3 MeV shown in Figure 1. Then the solenoid magnets focus and collimate the bunches, so that the pulse duration of compressing the bunch to the sample target is less than 50fs rms for pump-probe experiment [1]. To achieved this goal, it is vital for LLRF controller to satisfy the stability: ±0.01% (rms) for the amplitude and ±0.01° (rms) for the phase, respectively. Before the facility construction, the LLRF controller should be designed to achieve the necessary field regulation requirements [2].

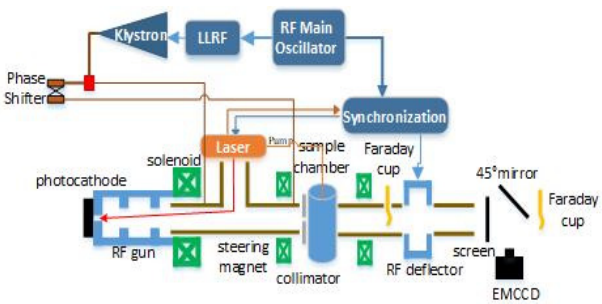

Figure 1: Overview of the UED.

* Work supported by the National Natural Science Foundation of China (NSFC) 11728508
† kjfan@hust.edu.cn

LONGITUDINAL MOTION

For LLRF, the difference in flight time is mainly caused by the following three aspects. First, the laser pulse jitter will make the electron emission time different. Second, the difference in bunch length will cause different flight time. Third, the RF phase jitter makes the particle flight time different.

$$\Delta t = \frac{\Delta\Phi}{\omega} = \frac{\Delta\Phi}{2\pi f} = \frac{\Delta\Phi}{2\pi \times 2.856 \times 10^9} \quad (1)$$

where requires time jitter $\Delta t = 50$ fs, $\Delta\Phi = 0.01°$.So, the LLRF should satisfy the stability: ±0.01° (rms) for the phase.

Assuming that the centre of the laser pulse with the length σ_i reaches the cathode surface at time t = 0, the bunch head and tail reach the cathode surface at times $-\sigma_i/2$ and $+\sigma_i/2$, respectively, and the corresponding electron microwave field emission phases are $\phi_0 - C\sigma_i/2$ and $\phi_0 + C\sigma_i/2$, respectively, where C is a constant that converts time into the phase of the microwave. Then the difference between the time when the bunch head and tail arrive the same position is expressed as [3]:

$$\begin{aligned}\sigma_f &= t_{tail} - t_{head} \\ &= [\frac{\sigma_i}{2} + T_f(\Phi_0 + \frac{C\sigma_i}{2})] - [-\frac{\sigma_i}{2} + T_f(\Phi_0 - \frac{C\sigma_i}{2})] \\ &= \sigma_i + T_f(\Phi_0 + \frac{C\sigma_i}{2}) - T_f(\Phi_0 - \frac{C\sigma_i}{2})\end{aligned} \quad (2)$$

The above formula can be approximated as:

$$\sigma_f = \sigma_i + C\sigma_i(\frac{dT_f}{d\Phi})_{\Phi=\Phi_0} \quad (3)$$

When the electric field amplitude $E_0 = 76$ MV/m, the electronic flight time T_f changes with the electron emission phase ϕ_0 ,which is shown in Figure 2.

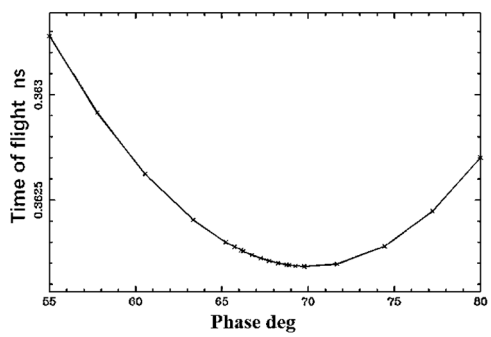

Figure 2: Time of flight measured versus electron emission phase during a phase scan.

The time when the laser reaches the cathode surface is defined as t = 0, and the phase in the microwave field at

ISBN: 978-3-95450-208-0 doi:10.18429/JACoW-IPAC2019-THPRB050

this time is ϕ_0, whereas in the actual experimental apparatus, there is the time synchronization jitter between the microwave signal and the laser pulse. While the synchronous jitter between the phase of the microwave field and the laser pulse is σ_{RL}, the electron is actually emitted from the cathode face at a phase of $\Phi_0 + C\sigma_{RL}$, and the jitter between it and the reference electron emitted nominally at ϕ_0 is:

$$\begin{aligned}\Delta T_{f,RL} &= T_f(\Phi_0 + C\sigma_{RL}) - T_f(\Phi_0) \\ &= C\sigma_{RL}\left(\frac{dT_f}{d\Phi}\right)_{\Phi=\Phi_0} \\ &= F_{ij}(\Phi_0)\sigma_{RL}\end{aligned} \tag{4}$$

The influence factor $F_{ij}(\phi_0)$ introduced here describes the given time jitter between the microwave field and the laser at the different phase ϕ_0, which ultimately leads to the arrival time jitter of the electrons, and it is the derivative of the time of flight $T_f(\phi_0)$. The position of $F_{ij} = 0$, that is, the T_f at this phase takes the extreme value, where the phase is 69.77°is shown in Figure 2.

LLRF CONTROLLER DESIGN

The schematic diagram of the LLRF system is shown in Figure 3. The RF system at UED consists of 1.4 cell RF gun and solenoid coil. Before its construction, it is crucial for us to build the system model to analyse.

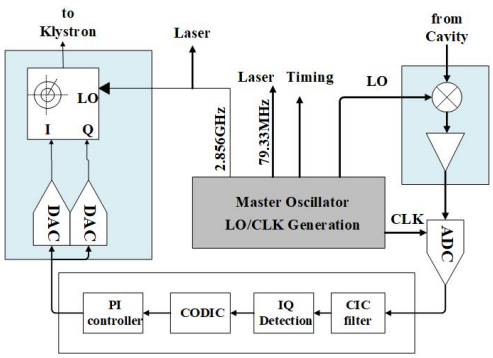

Figure 3: Overview of LLRF system.

Equivalent Circuit Model

In high-frequency electronic circuits, the input coupler can be equivalent to a transformer with a transformer ratio of 1: n. The cavity can be equivalent to an RLC resonant circuit, and the parameters in the circuit can be represented by voltage and current shown in Figure 4. The circuit is simplified to be equivalent to the circuit shown in Figure 5.

Cavity Model Simulation

The circuit can be analysed by the equivalent circuit on the resonant cavity side shown in Figure 5. The differential equation of the cavity voltage obtained by Kirchhoff's law in the circuit theory is:

$$\ddot{V}_c(t) + \frac{1}{RL}\dot{V}_c(t) + \frac{1}{LC}V_c(t) = \frac{1}{C}\dot{I}(t) \tag{5}$$

Using microwave parameters instead of circuit parameters can be obtained:

$$\ddot{V}_c(t) + \frac{\omega_0}{Q_L}\dot{V}_c(t) + \omega_0^2 V_c(t) = \frac{\omega_0 R_L}{Q_L}\dot{I}(t) \tag{6}$$

In LLRF systems, high-power input and output signals are typically RF signals of a certain frequency. The voltage and current can be expressed as:

$$\begin{aligned}V_c(t) &= (V_r(t) + jV_i(t))e^{j\omega t} \\ I(t) &= (I_r(t) + jI_i(t))e^{j\omega t}\end{aligned} \tag{7}$$

where ω is the oscillating angular frequency of the RF signal. Bringing the differential equation to the equation, and opening the virtual part of the real part, the final simplification can be obtained [3]:

$$\begin{aligned}\dot{V}_r + \Delta\omega V_i + \omega_h V_r &= \omega_h R_L I_r \\ \dot{V}_i - \Delta\omega V_r + \omega_h V_i &= \omega_h R_L I_i\end{aligned} \tag{8}$$

Then the cavity model built with MATLAB/Simulink is shown in Figure 6.

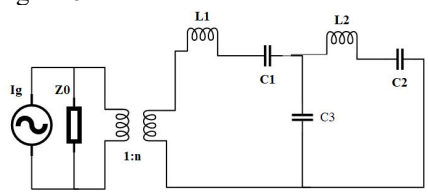

Figure 4: 1.4 cell RF gun equivalent circuit.

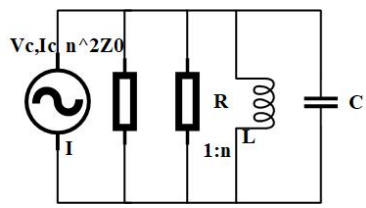

Figure 5: Equivalent circuit after simplification.

High-Voltage Modulator Fluctuation

Fluctuations in the high voltage modulator affect the amplitude and phase of the klystron output signal. Voltage fluctuations cause a change in the amplitude of the klystron output signal. The relationship between the amplitude and the klystron cathode voltage is as follows [4]:

$$\frac{dV_{out}}{V_{out}} = \frac{5}{4}\frac{dV}{V} \tag{9}$$

Assuming that the klystron output signal is cos(ωt), the cathode voltage ripple of klystron is ΔV. The amplitude fluctuation and phase fluctuation of the RF output signal can be expressed as ΔA and Δθ. The klystron gain is A, then its output signal can be expressed as:

$$V_{out} = (A + \Delta A)\cos(\omega t + \Delta\theta) \tag{10}$$

Considering relativity, it can be obtained:

$$\begin{aligned}d\theta &= -\frac{e\omega L}{mc^3\beta^3\gamma^3}dV \\ &= -\frac{e\omega LV}{mc^3\beta^3\gamma^3}\frac{dV}{V}\end{aligned} \tag{11}$$

ISBN: 978-3-95450-208-0 doi:10.18429/JACoW-IPAC2019-THPRB050

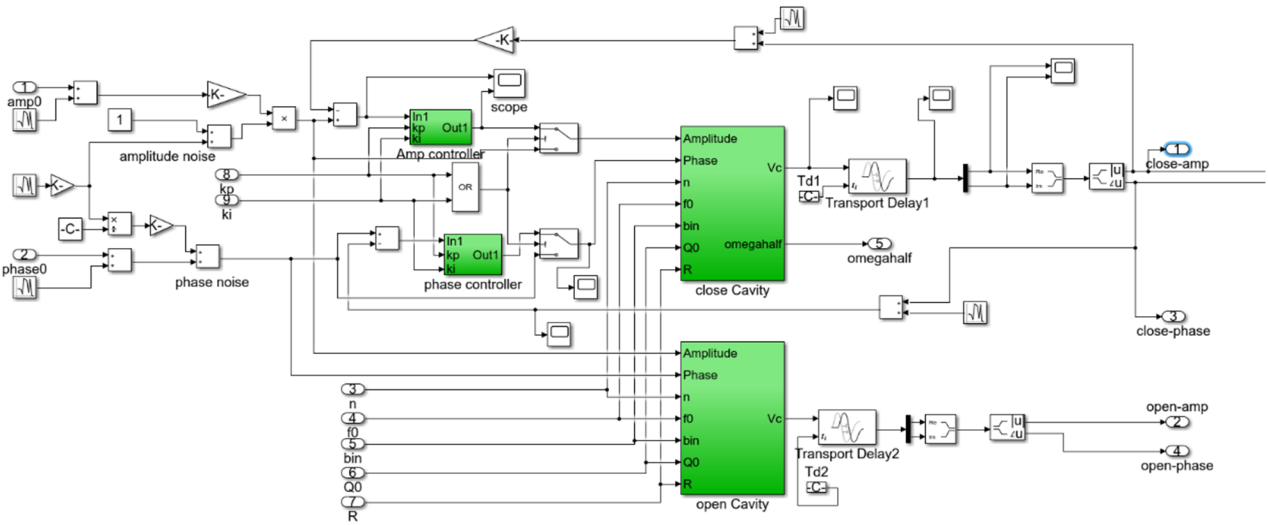

Figure 6: LLRF system simulated in MATLAB/Simulink, where work frequency $f_0 = 2856$ MHz, cavity quality factor $Q_0 = 12000$, cavity input coupling $\beta_0 = 0.9$.

PI Controller

The RF cavity is a first order low pass filter in base-band (assume that it is operated on-resonance). Then the cavity with half bandwidth $\Omega_{0.5}$ can be expressed as [5]:

$$H_{cavity}(s) = \frac{\Omega_{0.5}}{s + \Omega_{0.5}} \tag{12}$$

The suppression of the disturbance signal by the LLRF system is affected by the open-loop gain L(s) (open-loop transfer function), which is manifested as follows: the larger the open-loop gain, the stronger the disturbance suppression capability. However, a large open-loop gain can cause system instability, which is a contradiction between loop anti-disturbance performance and stability margin. The open loop transfer function of the whole system is as follows:

$$\begin{aligned} L(s) &= G \cdot H_{cavity} \cdot E(s) \\ &= G \cdot \left(\frac{\Omega_{0.5}}{s + \Omega_{0.5}}\right) \cdot e^{-sT_d} \end{aligned} \tag{13}$$

where E(s) is the delay module, T_d is the total delay, including the digital delay caused by the internal digital signal processing algorithm in the FPGA, the analogy delay caused by the cable and other devices. The general delay T_d is 1-1.5μs.

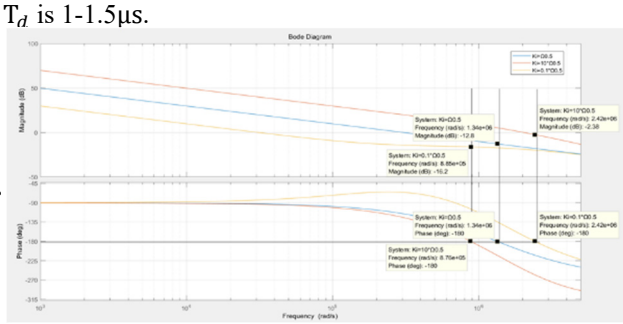

Figure 7: Bode plots of LLRF system.

In MATLAB simulation, the Pade function is needed to approximate the loop delay module. The bode plots is shown in Figure 7. Then we can predict the system stability of the LLRF system of the cavity by its Bode plots. The system performance was measured and evaluated via different proportional gain K_P and integral gain K_I. After gain-scanning, it can be obtained that $K_P = 0.1$, $K_I = 1000$.

Stabilities of LLRF

The typical LLRF system performance and parameters during experiment are listed above. The feedback gains were determined by the PI controller tuning, as stated above. Disturbing signals such as power supply ripples and microphonics can be suppressed well in the model shown in Figure 8.

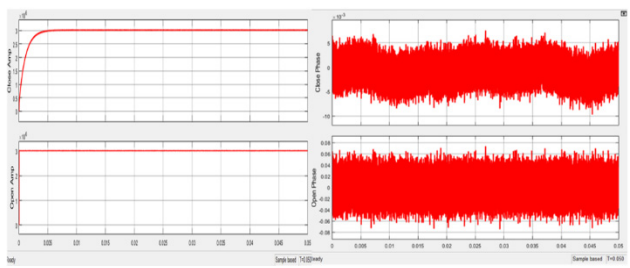

Figure 8: Operation results of LLRF system.

CONCLUSION

The basic design of the LLRF system for the HUST UED machine has been simulated. All of the simulated results show good performance to satisfy the fifty femtoseconds accuracy. The simulation of the LLRF system in UED can provide theoretical support for the construction of the whole UED system. We will improve the algorithm to satisfy the better precision.

ISBN: 978-3-95450-208-0 doi:10.18429/JACoW-IPAC2019-THPRB050

REFERENCES

[1] M. Titberidze *et al*., "Present and Future Optical-to-Microwave Synchronization Systems at REGAE Facility for Electron Diffraction and Plasma Acceleration Experiments", in *Proc. 6th Int. Particle Accelerator Conf. (IPAC'15)*, Richmond, VA, USA, May 2015, pp. 833-836. doi: 10.18429/JACoW-IPAC2015-MOPHA026

[2] M. Hoffmann *et al*., "Precision LLRF Controls for the S-Band Accelerator REGAE", in *Proc. 4th Int. Particle Accelerator Conf. (IPAC'13)*, Shanghai, China, May 2013, paper WEPME008, pp. 2938-2940.

[3] X.Wang, X. Qiu, I. Ben-Zvi, "Experimental observation of high-brightness microbunching in a photocathode rf electron gun", *Phys. Rev. E,* vol. 54, no. 4, pp. R3121-R3124, Oct. 1996. doi: 10.1103/PhysRevE.54.R3121

[4] C. Schmidt, "RF System Modeling and Controller Design for the European XFEL", Ph.D. thesis, Technischen Universit¨at Hamburg-Harburg, Hamburg, Germany, 2010.

[5] F. Qiu *et al*., "A Disturbance-Observer-based Controller for LLRF Systems", in *Proc. 6th Int. Particle Accelerator Conf. (IPAC'15)*, Richmond, VA, USA, May 2015, pp. 2895-2898. doi: 10.18429/JACoW-IPAC2015-WEPMA054